sustainability

MDPI

Article

Operator Protection from Gamma Rays Using Ordinary Glass and Glass Doped with Nanoparticles

Muhammad Zubair [1,2,*], Muhammad Aamir [3,*], Eslam Ahmed [2] and Abdullrahman Abdullah Alyemni [4]

[1] Department of Mechanical & Nuclear Engineering, University of Sharjah, Sharjah P.O. Box 27272, United Arab Emirates
[2] Research Institute of Sciences and Engineering, University of Sharjah, Sharjah P.O. Box 27272, United Arab Emirates
[3] Department of Basic Sciences, Deanship of Preparatory Year, King Faisal University, Hofuf 31982, Saudi Arabia
[4] College of Engineering, King Faisal University, Hofuf 31982, Saudi Arabia
* Correspondence: mzubair@sharjah.ac.ae (M.Z.); msadiq@kfu.edu.sa (M.A.)

Abstract: Radiation-shielding glass is utilized in a few applications such as nuclear medicine, (PET) scans, x-rays, or treatment use. Nuclear reactors additionally require shielding from radiation types such as gamma, x-rays, and neutron emissions. Radiation-shielding glass is additionally utilized in the exploration and industry fields, for example, in cyclotron support testing of non-destructive materials, and the improvement of airport x-ray machines. Notwithstanding, radiation-shielding glass utilizes space innovation to protect both the astronauts and tools from cosmic rays. Nanoparticles have been involved recently in those applications. Several simulations using MCNP 6 have been used in this study to compare a variety of conventional and nanoparticle-doped glass, including silicate glass (containing BiO or PbO), BZBB5, and glass containing nanoparticles, including $Na_2Si_3O_7$/Ag, $Al_2H_2Na_2O_{13}Si_4$/HgO, and lead borate glass containing ZrO_2 to detect shielding properties for operators at different gamma energies. We investigated the percentage of transmitted photons, linear attenuation coefficient, half-value layer, and mean free path for the selected glass. Several shielding properties were not significantly different between the simulated results and the theoretical data available commercially. Based on the results, those parameters depend on the glass material due to their densities and atomic number. It has been found that 70 Bismuth(III) oxide:30 Silica has the best shield properties from gamma rays, such as a low percentage of transmitted photons, low HVL, and low MFP, which is due to its high density and atomic number.

Keywords: radiation protection; nanoparticles; nuclear applications; percentage of the transmitted photons; half-value layer; linear attenuation coefficient; mean free path; Monte Carlo simulation

Citation: Zubair, M.; Aamir, M.; Ahmed, E.; Alyemni, A.A. Operator Protection from Gamma Rays Using Ordinary Glass and Glass Doped with Nanoparticles. *Sustainability* **2023**, *15*, 1375. https://doi.org/10.3390/su15021375

Academic Editors: Moussa Leblouba, Balaji PS, Muhammad Rahman, Brabha Nagaratnam, Keerthan Poologanathan and Changhyun Roh

Received: 17 November 2022
Revised: 28 December 2022
Accepted: 5 January 2023
Published: 11 January 2023

1. Introduction

Nuclear energy, which now generates 13% of the world's electrical output, has emerged as a crucial alternative in the search for sustainable energy sources as it becomes imperative in the modern world to replace fossil fuels [1,2]. In addition, nuclear energy is not only limited to the production of electricity, but X-rays and gamma-rays also are good for penetrating and detecting opaque materials due to their short wavelength (high energy), and they have constant energy levels for each isotope, which can be used to identify unknown radioactive sources [3,4]. Gamma radiation is most commonly used in medical equipment, such as sterile dressings, tubes, catheters, needles, implantation assembly, and embeds [5]. In the food business, gamma radiation is also used to dry natural commodities, including fruits, vegetables, herbs, and meat.

Lead glass and other forms of specialty glass are now deemed essential for radiation protection. The lead-containing glass absorbs different forms of radiation, such as gamma, x-ray, and neutron radiation. Because of this unique mix of properties, glass is an essential

radiation barrier for applications that need a view, such as clinical radiography and nuclear fuel processing. In different locations, radiation-shielding glass screens and windows are used to protect medical care operators and experts from x-ray and gamma-ray sources such as spectrometers, computed tomography (CT) scanners, and positron emission tomography (PET) [6].

Other forms of heavy metal oxide (HMO) modifiers used in radiation-shielding glass include lead oxide (PbO) and bismuth oxide (Bi_2O_3). Using these chemical compounds, regular silicate glass may be transformed into transparent radiation shields that protect operators from neutrons, gamma rays, and x-rays. While allowing visible light to cross through, the resultant glass may attenuate radiation to levels equivalent to concrete and other popular shielding materials [7]. Because of environmental concerns regarding lead consumption, many HMO glass varieties have been developed for radiation shielding applications. Boron, tellurium, barium, and silicon oxides are among them [8,9]. According to some studies, these glasses might eventually replace conventional concrete as gamma-ray shielding materials.

Radiation-shielding glass is used extensively in nuclear medicine, for example, PET scans use radioactive materials or sources (such as radiation therapy). As a result, radiation-shielding glass is commonly employed to allow operators to handle radioactive material while avoiding potentially dangerous radiation exposure. Effective radiation shielding is essential in the nuclear industry. In waste reprocessing for nuclear reactors and laboratory uses, radiation-shielding glass windows can be utilized to allow operators to safely inspect radioactive materials during processing. Radiation-shielding glass is utilized in various scientific and industrial applications, including cyclotron maintenance, testing of non-destructive materials, and the development of airport x-ray equipment. In order to protect astronauts and equipment from cosmic rays, which are created from photons and particles from outside the solar system or from the sun and intensify during solar flare (or "sun storm") periods, glass is also utilized in spacecrafts [10,11].

The development of radiation sensors, detectors, radiation shielding materials, and in-service monitors using nanotechnology has also made it possible to monitor for radiation, temperature, pressure, in situ diagnostics of material properties and mechanical response, corrosion, neutron flux, strain, or even chemistry with little impact on system execution, leading to a fundamental increase in sensitivity and a decrease in the size and weight of the system with little impact on performance [12]. For the use of nanoparticles in radiation shielding, several studies have been conducted to test and propose new materials, such as silicone rubbers doped with nanoparticles or different types of glass doped with nanoparticles [13–18].

2. Materials and Methods

Due to the world's evolution, nanoparticles have been used in radiation protection by doping them with different types of glass, which will improve electric or dielectric, mechanical, optical, electronic, and surface properties. Recently, several researchers have switched from ordinary glass to shielding glass in high radiation areas, such as space, medical institutes, and nuclear power plants. This paper compares some of these gamma-ray-shielding glasses. Two types of glass have been investigated in this paper, a silicate glass containing BiO or PbO [14], BZBB5 [15] and a glass doped with nanoparticles. Table 1 shows a variety of glass densities and elemental fractions for this investigation, including glass doped with nanoparticles such as $Na_2Si_3O_7$/Ag [16], $Al_2H_2Na_2O_{13}Si_4$/HgO [17], and lead borate glass doped with ZrO_2 [18]. Because they are the densest samples in their group, they scatter more photons because they scatter more light.

Table 1. Properties of suggested material.

Glass	Density (g/(cm)^3)	Elemental Fraction
Conventional Glass		
BZBB5	6.15	Zn: 0.321369; O: 0.31643; Bi: 0.224247; B: 0.093171; Ba: 0.044783
70 Bi_2O_3:30 SiO_2	5.69	O: 0.125519; Si: 0.024494; Bi: 0.849987
70 PbO:30 SiO_2	4.93	O: 0.119337; Si: 0.048333; Pb: 0.832330
Glass Doped With Nanoparticles		
$Na_2Si_3O_7$/Ag	2.012	Na: 0.2711; O: 0.0656; Si: 0.5533; Ag: 0.11
$Al_2H_2Na_2O_{13}Si_4$/HgO	3.647	Hg: 0.3705; Al: 0.0767; H: 0.0029; Na: 0.0635; O: 0.3251; Si: 0.1596
Lead Borate Glass Doped with ZrO_2	5.29	Zr: 0.17768; O: 0.40077; Na: 0.12796; B: 0.12035; Pb: 0.17325

According to their fields, operators behind the glass sample are exposed to different energies of gamma rays. A NaI(Tl) detector measuring "2 × 2" and various isotropic radioactive point sources, including I-131, Cs-137, and Co-60, is included in the simulation setup, as seen in Figure 1. These sources release gamma rays with energy ranging from 0.36 to 0.66 to 1.17 to 1.33 MeV. Astronauts in spacecrafts are exposed to these sources, as well as extremely high energy sources (5MeV and 10 MeV), from gamma-ray bursts, blazars, and pulsars, which will require very thick shielding materials due to the loss the most of the photons' energy before being exposed to the astronauts [19,20]. However, due to unifying our shielding thickness for all studied materials, we used the same thickness over the whole range of energies. Each source is on the other side of the glass sample, on the horizontal plane. The glass sample can be made from any of the varieties of glass specified in Table 1.

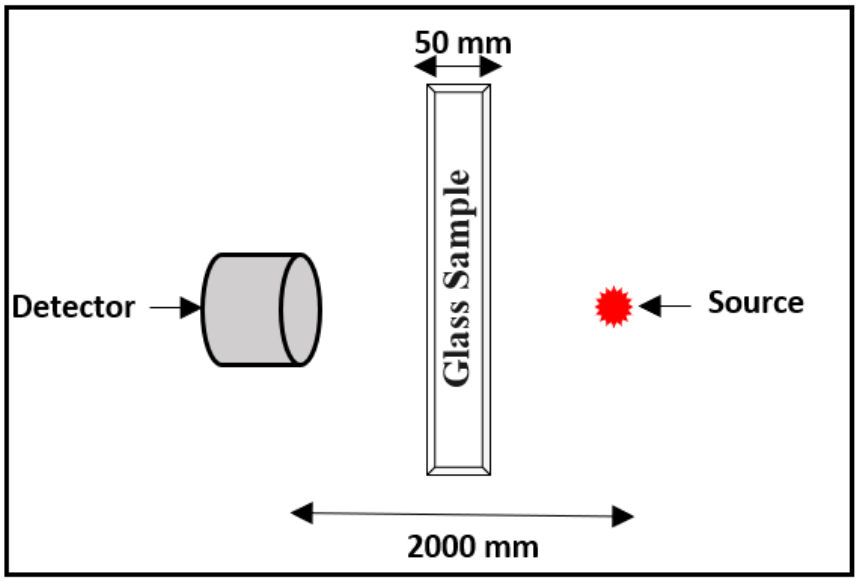

Figure 1. Simulation setup.

This setup simulates a scenario in which an operator in a medical institute or a nuclear power plant or an astronaut in a spacecraft will be operating a detector and various radioactive sources emitting gamma rays with different energies of 0.36, 0.66, 1.17, 1.33, 5, and 10 MeV depending on the source. To protect the operators, a glass sample 500 mm × 1000 mm in dimension and 50 mm in thickness was placed between the source and detector at a separation distance of 2000 mm, and the composition of the glass sample could be any of the materials listed in Table 1. Since a gamma source is utilized in the simulations, it is possible to ignore the air in the surrounding volume because there is minimal interaction with it. Nevertheless, this volume is crucial.

Three critical parameters should be compared between ordinary glass and glass doped with nanoparticles, starting with Monte Carlo N-Particle (MCNP) simulations of six different glass shielding materials. After that, data analysis must be conducted as depicted in Figure 2 in order to obtain the required shielding properties. The half-value layer (HVL), which represents the thickness of the absorber that will reduce the gamma rays to half, the mean free path (MFP), which is the average dispersion, and the percentage of photons transmitted, which is required to comprehend how the shield glass affects the number of photons transmitted depending on their density and material, are all components of the linear attenuation coefficient.

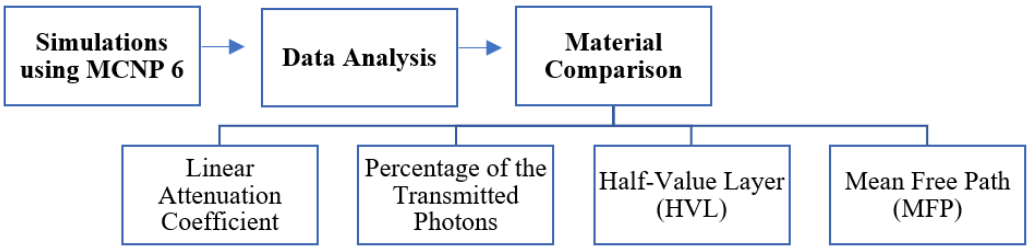

Figure 2. Methodology of the research.

Numerous simulations were conducted using MCNP 6.2 and the ENDF/B-VII libraries to determine the properties of the glass that would protect the operators [21]. The NaI detector response was measured using the pulse height tally (F8), which has 1024 energy bins. Three unique radioactive sources were employed throughout the simulations, and the shielding glass sample was made from six different materials. In contrast, the glass had the same thickness and size, and each simulation used a total of 1 billion histories to determine the degree of shielding for each sample.

With the major objectives of determining the percentage of transmitted photons, the half-value layer, and the mean free path, investigations on the spectra obtained at various glass materials were carried out. The equation for the main source photons provided below can be used to calculate the percentage of photons that are transferred [22].

$$\frac{I}{I_0}(\%) = e^{-\mu t} \times 100(\%) \quad (1)$$

where the linear attenuation coefficient (μ) is used. The number of photons (I) that are transmitted from a glass shield with the thickness (t) is expressed in terms of the number of photons (I_0) that are not protected by a glass shield.

The mean free path and the half-value layer are given by the following:

$$HVL\ (cm) = \frac{ln(2)}{\mu} \quad (2)$$

$$MFP\ (cm) = \frac{1}{\mu} \quad (3)$$

The mean free path and the half-value layer are determined from the simulations utilizing the linear attenuation coefficient calculated from the transmitted photons from each glass sample.

3. Results and Discussions

As noted above, several simulations were probably run to compare the various materials for shielding operators in various fields from gamma rays at varying energy. One of the parameters used in this study to estimate the probability of the shield interacting with photons was the linear attenuation coefficient. Based on theoretical predictions for various shielding materials, the linear attenuation coefficient was computed using XCOM [23]. The outcomes of several simulations ran using MCNP 6.2 are displayed in Tables 2 and 3 below that show that the probability of attenuated photons at low energies rises with the square of the shield's atomic number and falls with the gamma-ray energy since photo-absorption is more likely at lower energies [24].

Table 2. Comparison of theoretical and simulated linear attenuation coefficients (cm^{-1}).

Glass Sample	0.36 MeV		0.66 MeV		1.17 MeV		1.33 MeV		5 MeV		10 MeV	
	Theo.	Sim.	Theo.	Sim.	Theo.	Sim.	Theo.	Sim.	Theo.	Sim.	Theo.	Sim.
70 Bi_2O_3:30 SiO_2	1.47	1.43	0.59	0.59	0.35	0.36	0.32	0.31	0.23	0.23	0.26	0.25
70 PbO:30 SiO_2	1.22	1.21	0.50	0.49	0.30	0.31	0.27	0.27	0.19	0.20	0.22	0.21
BZBB5	0.88	0.84	0.51	0.51	0.35	0.37	0.33	0.32	0.20	0.20	0.19	0.19
Lead borate glass doped with ZrO_2	0.67	0.66	0.42	0.42	0.30	0.32	0.28	0.28	0.16	0.16	0.15	0.14
$Al_2H_2Na_2O_{13}Si_4$/HgO	0.59	0.56	0.32	0.31	0.22	0.23	0.20	0.19	0.12	0.12	0.12	0.11
$Na_2Si_3O_7$/Ag	0.20	0.19	0.15	0.15	0.12	0.13	0.11	0.10	0.06	0.05	0.05	0.05

Table 3. Comparison of theoretical and simulated percentage of transmitted photons.

Glass Sample	0.36 MeV		0.66 MeV		1.17 MeV		1.33 MeV		5 MeV		10 MeV	
	Theo.	Sim.	Theo.	Sim.	Theo.	Sim.	Theo.	Sim.	Theo.	Sim.	Theo.	Sim.
70 Bi_2O_3:30 SiO_2	0.06	0.08	5.16	5.25	17.73	16.5	20.60	20.8	31.32	31.1	27.09	28.4
70 PbO:30 SiO_2	0.22	0.22	8.17	8.47	22.76	20.9	25.79	26.3	37.12	36.8	32.98	34.3
BZBB5	1.25	1.54	7.97	7.94	17.15	15.9	19.40	19.7	36.57	36.2	37.95	38.5
Lead borate glass doped with ZrO_2	3.55	3.59	12.06	12.0	21.87	19.8	24.19	24.6	44.24	44.4	48.06	49.1
$Al_2H_2Na_2O_{13}Si_4$/HgO	5.33	6.00	20.47	20.7	34.05	31.5	36.81	37.6	54.21	53.9	55.49	57.8
$Na_2Si_3O_7$/Ag	36.26	37.1	46.49	46.5	55.99	51.9	58.10	58.5	74.23	75.1	77.65	79.1

The percentage of transmitted photons should be taken into account while defining shielding materials. There are two ways to select this parameter, as illustrated in Figure 3. The first technique calculates the photon intensity ratio with and without the shield at various energies using simulations. The second technique computes the percentage of transmitted photons based on the linear attenuation coefficient obtained from XCOM using Equation (1). High-density materials, such as 70 Bismuth(III) oxide:30 Silica, have the lowest percentage of transmitted photons, which is close to 0% at low energies, as seen in Figure 3a,b due to their high linear attenuation coefficient, as previously mentioned. On the other hand, low-density materials, such as $Na_2Si_3O_7$/Ag, have a high percentage of transmitted photons, especially at high energies, due to their low linear attenuation coefficient.

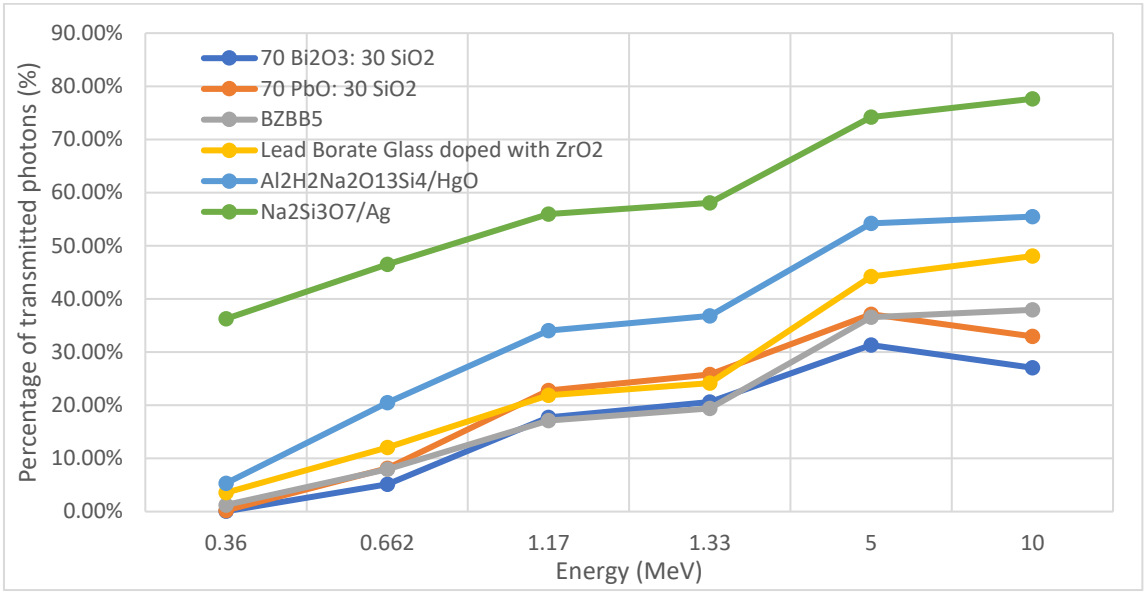

(**a**)

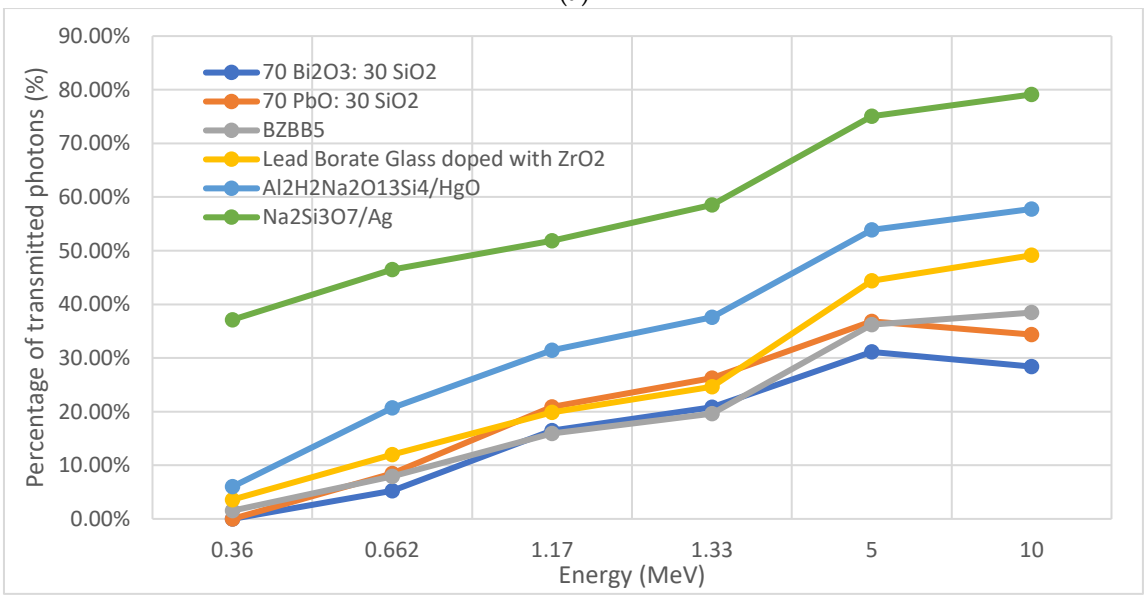

(**b**)

Figure 3. (**a**) Theoretical percentage of transmitted photons; (**b**) Simulated percentage of transmitted photons.

HVL is a crucial parameter for comparing the shielding performance of materials since different materials attenuate radiation to different degrees. Table 4 lists the HVL for the six shielding materials, representing the material thickness that will attenuate half of the gamma rays [25]. As shown in Figure 4a,b, the low-density materials and high energy sources have high HVL, which means that they will require more material thickness to attenuate the gamma rays completely, which is also concluded from the percentage of transmitted photons for the low-density materials and high-energy sources. Especially for $Na_2Si_3O_7$/Ag glass for the energies above 1.33 MeV, it shows an extreme increase in the percentage of transmitted photons, and this clearly indicates that this material does not attenuate photons with high effectiveness at high energies due to the low value of the linear attenuation coefficient at those energy ranges for this material, which are less than 0.1 cm^{-1}.

Table 4. Comparison of theoretical and simulated HVL (cm).

Glass Sample	0.36 MeV		0.66 MeV		1.17 MeV		1.33 MeV		5 MeV		10 MeV	
	Theo.	Sim.	Theo.	Sim.	Theo.	Sim.	Theo.	Sim.	Theo.	Sim.	Theo.	Sim.
70 Bi_2O_3:30 SiO_2	0.47	0.49	1.17	1.18	2.00	1.92	2.19	2.21	2.99	2.97	2.65	2.75
70 PbO:30 SiO_2	0.57	0.57	1.38	1.40	2.34	2.21	2.56	2.59	3.50	3.47	3.12	3.25
BZBB5	0.79	0.83	1.37	1.37	1.97	1.88	2.11	2.13	3.45	3.41	3.58	3.63
Lead borate glass doped with ZrO_2	1.04	1.04	1.64	1.63	2.28	2.14	2.44	2.47	4.25	4.27	4.73	4.88
$Al_2H_2Na_2O_{13}Si_4$/HgO	1.18	1.23	2.19	2.20	3.22	3.00	3.47	3.54	5.66	5.60	5.88	6.32
$Na_2Si_3O_7$/Ag	3.42	3.50	4.52	4.52	5.98	5.28	6.38	6.47	11.63	12.1	13.70	14.8

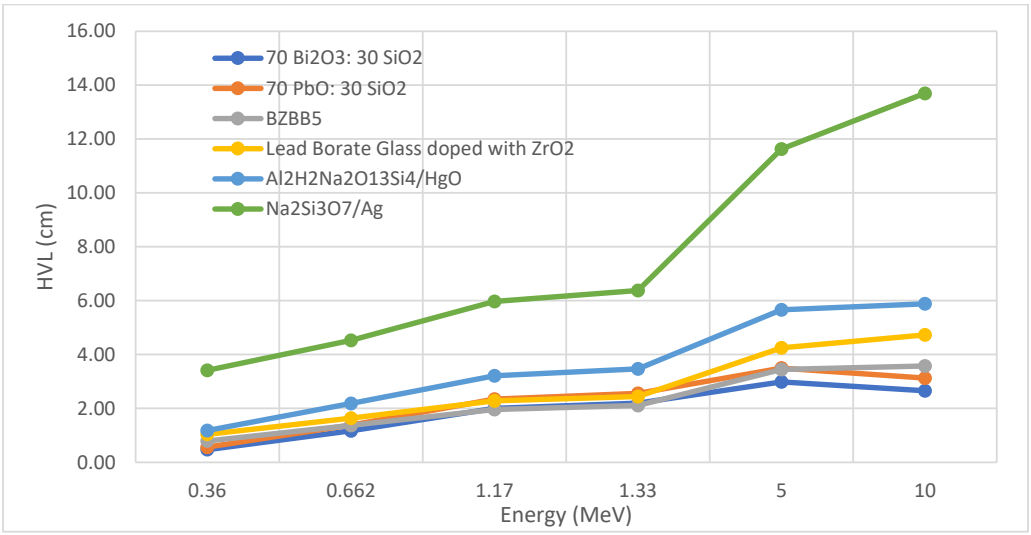

(**a**)

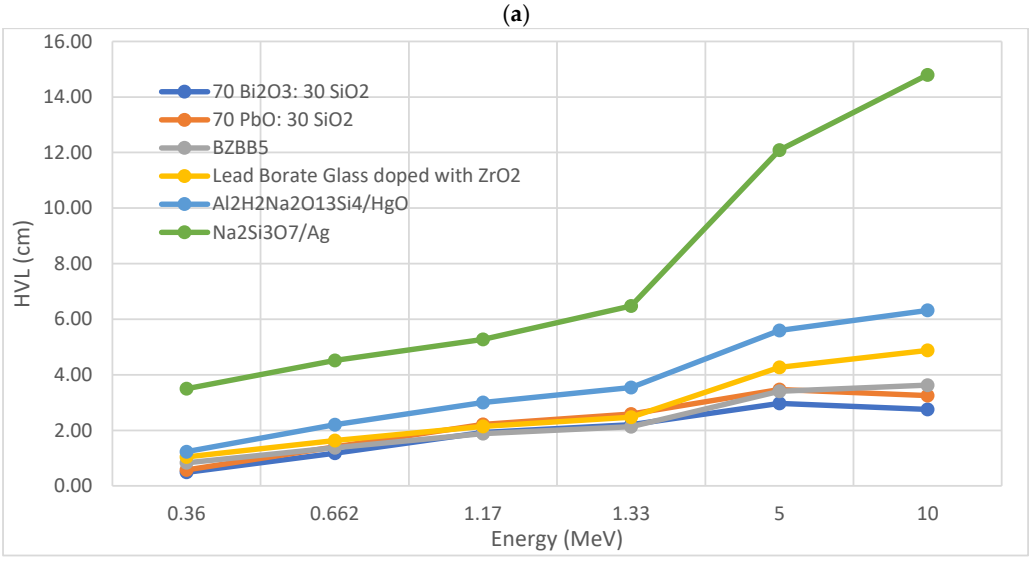

(**b**)

Figure 4. (**a**) Theoretical half-value layer, (**b**) Simulated half-value layer.

MFP is the opposite of the linear attenuation coefficient and, with a lower value, means a more effective material. Table 5 shows MFP for the selected materials, which describes the average distance of the particles before the interactions [26]. As shown in Figure 5a,b, the low-density materials and high-energy sources have high MFP, which means the particles

cross the materials for high distances before interacting with the low-density materials and high energy source, which is also concluded from the percentage of transmitted photons and HVL above for those materials at high-energy sources.

Table 5. Comparison of theoretical and simulated MFP (cm).

Glass Sample	0.36 MeV		0.66 MeV		1.17 MeV		1.33 MeV		5 MeV		10 MeV	
	Theo.	Sim.	Theo.	Sim.	Theo.	Sim.	Theo.	Sim.	Theo.	Sim.	Theo.	Sim.
70 Bi_2O_3:30 SiO_2	0.68	0.70	1.69	1.70	2.89	2.77	3.16	3.18	4.31	4.28	3.83	3.97
70 PbO:30 SiO_2	0.82	0.83	2.00	2.03	3.38	3.19	3.69	3.74	5.05	5.00	4.51	4.68
BZBB5	1.14	1.20	1.98	1.97	2.84	2.72	3.05	3.07	4.97	4.92	5.16	5.23
Lead borate glass doped with ZrO_2	1.50	1.50	2.36	2.36	3.29	3.09	3.52	3.57	6.13	6.16	6.82	7.04
$Al_2H_2Na_2O_{13}Si_4$/HgO	1.71	1.78	3.15	3.17	4.64	4.32	5.00	5.11	8.17	8.08	8.49	9.11
$Na_2Si_3O_7$/Ag	4.93	5.05	6.53	6.52	8.62	7.61	9.21	9.34	16.78	17.4	19.76	21.4

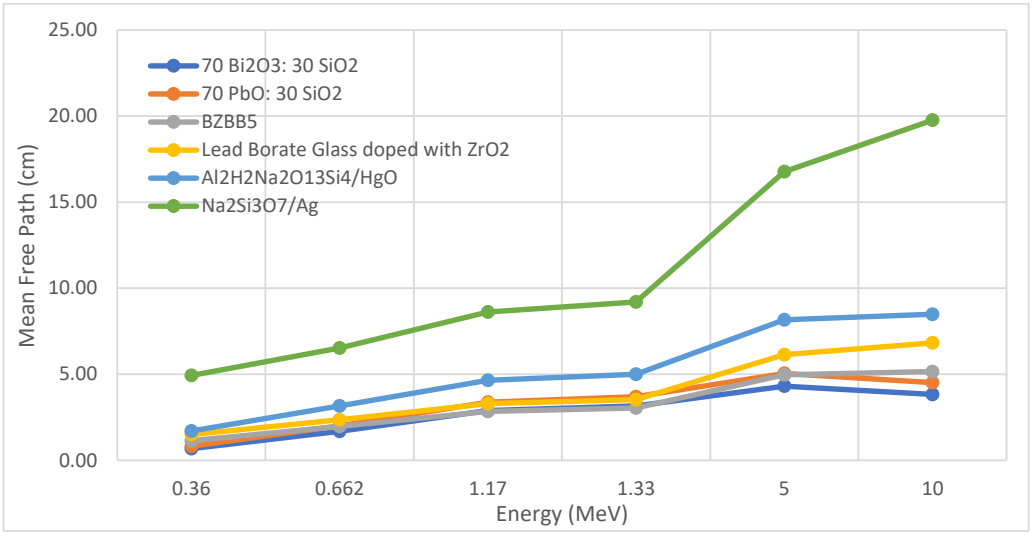

(**a**)

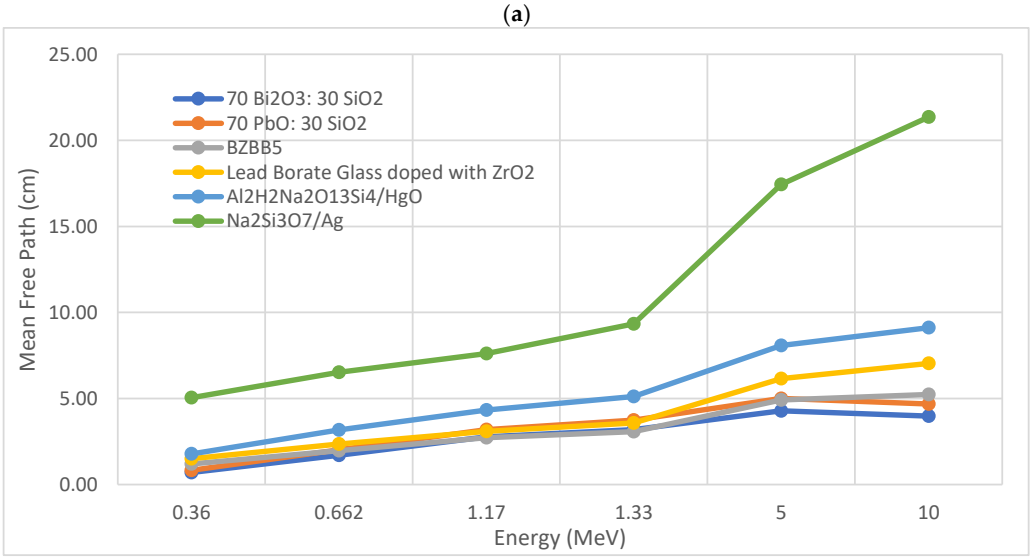

(**b**)

Figure 5. (**a**) Theoretical mean free path; (**b**): Simulated mean free path.

4. Conclusions

Applications for radiation-shielding glass include nuclear medicine, such as (PET) scans, x-rays, or therapeutic usage. Gamma, x-ray, and neutron outputs are more radiation types that nuclear reactors need to be protected from. Additionally, radiation-shielding glass is employed in a variety of academic and industrial settings, including cyclotron maintenance, non-destructive material testing, and the creation of airport *x*-ray equipment. In addition to protecting equipment and astronauts from gamma rays in spacecrafts.

Nanoparticles have lately been used in several applications. Radiation-shielding glass has been made from a variety of materials, including regular glass and glass with nanoparticles. In this study, numerous glass materials that were both doped and not doped with nanoparticles were reviewed and simulated. As shown in Tables 2–5, the shielding characteristics of various kinds were calculated using XCOM and MCNP 6. Operators in the various applications will be shielded against gamma energy of 0.36, 0.66, 1.17, 1.33, 5 and 10 MeV using these various glasses with the same thickness and dimensions.

Simulated findings showed a clear separation between common glasses, such as silicate glass (including lead(II) oxide or BiO) and BZBB5, and nanoparticle glasses, such as $Na_2Si_3O_7/Ag$, $Al_2H_2Na_2O_{13}Si_4/HgO$, and lead(II)-oxide-doped lead borate glass. According to the linear attenuation coefficients at all energies, the glass with a ratio of 70 bismuth(III) oxide to 30 silica transmits the minimum photons. These results are because this material has a high linear attenuation coefficient and a high density of the glass, which causes a decrease in the number of photons transmitted. We continue to work on this study to incorporate various materials for both regular and doped glass by simulations and experiments to give operators the most protection in various applications from different types of radiation.

Author Contributions: Conceptualization, M.Z.; methodology, M.Z. and E.A.; software, E.A.; validation, E.A. and M.Z.; writing—original draft preparation, M.Z. and E.A.; writing—review and editing, M.A. and A.A.A.; supervision, M.Z.; project administration, M.Z.; funding acquisition, M.A. and M.Z. All authors have read and agreed to the published version of the manuscript.

Funding: This research was funded by Deanship of Scientific Research, Vice Presidency for Graduate Studies and Scientific Research, King Faisal University, Saudi Arabia [Grant No. 2157] and the Research Institute of Science and Engineering at the University of Sharjah provided partial financing and support for Project Number Ref. V.C.R.G/ R.1325/2021.

Institutional Review Board Statement: Not applicable.

Informed Consent Statement: Not applicable.

Data Availability Statement: The research data is available on request.

Acknowledgments: This work was supported by the Deanship of Scientific Research, Vice Presidency for Graduate Studies and Scientific Research, King Faisal University, Saudi Arabia [Grant No2157]. The Research Institute of Science and Engineering at the University of Sharjah provided partial financing and support for Project Number Ref. V.C.R.G/ R.1325/2021, which the authors gratefully acknowledge.

Conflicts of Interest: The authors declare no conflict of interest.

References

1. Daghbouj, N.; Sen, H.S.; Callisti, M.; Vronka, M.; Karlik, M.; Duchoň, J.; Čech, J.; Havránek, V.; Polcar, T. Revealing nanoscale strain mechanisms in ion-irradiated multilayers. *Acta Mater.* **2022**, *229*, 117807. [CrossRef]
2. Daghbouj, N.; Sen, H.S.; Čížek, J.; Lorinčí, J.; Karlik, M.; Callisti, M.; Čech, J.; Havránek, V.; Li, B.; Krsjak, V.; et al. Characterizing heavy ions-irradiated Zr/Nb: Structure and mechanical properties. *Mater. Des. J.* **2022**, *219*, 110732. [CrossRef]
3. Bray, D.E.; Stanley, R.K. *Military Handbook: Nondestructive Evaluation: A Tool in Design, Manufacturing and Service*; CRC Press: Boca Raton, FL, USA, 2018.
4. Nasrazadani, S.; Hassani, S. Modern analytical techniques in failure analysis of aerospace, chemical, and oil and gas industries. In *Handbook of Materials Failure Analysis with Case Studies from the Oil and Gas Industry*; Elsevier: Amsterdam, The Netherlands, 2016.

5. Sandle, T.; Saghee, M.R. Some considerations for the implementation of disposable technology and single- use systems in biopharmaceuticals. *J. Commer. Biotechnol.* **2011**, *17*, 319–329. [CrossRef]
6. Zubair, M.; Ahmed, E.; Hartanto, D. Comparison of different glass materials to protect the operators from gamma-rays in the PET using MCNP code. *Radiat. Phys. Chem. J.* **2022**, *190*, 109818. [CrossRef]
7. Manohara, S.R.; Hanagodimath, S.M.; Gerward, L. Photon interaction and energy absorption in glass: A transparent gamma-ray shield. *J. Nucl. Mater.* **2009**, *393*, 465–472. [CrossRef]
8. Lakshminarayana, G.; Dong, M.G.; Al-Buriahi, M.S.; Kumar, A.; Lee, D.E.; Yoon, J.; Park, T. B^2O^3–Bi^2O^3–TeO^2–BaO and TeO^2–Bi^2O^3–BaO glass systems: A comparative assessment of gamma-ray and fast and thermal neutron attenuation aspects. *Appl. Phys. A* **2020**, *126*, 1–18. [CrossRef]
9. Singh, K.J.; Kaur, S.; Kaundal, R.S. Comparative study of gamma-ray shielding and some properties of PbO-SiO^2-$Al2O^3$ and Bi2O3-SiO2-Al2O3 glass systems. *Radiat. Phys. Chem.* **2014**, *96*, 153–157. [CrossRef]
10. Manonara, S.R.; Hanagodimath, S.M.; Gerward, L.; Mittal, K.C. Exposure buildup factors for heavy metal oxide glass: A radiation shield. *J. Korean Phys. Soc.* **2011**, *59*, 2039–2042. [CrossRef]
11. Bagshaw, M.; Barbeau, D.N. Chapter 44—The Aircraft Cabin Environment. In *Travel Medicine*, 3rd ed.; Elsevier: Amsterdam, The Netherlands, 2013; Available online: https://www.sciencedirect.com/science/article/pii/B9781455710768000442 (accessed on 27 December 2022).
12. Khanal, L.R.; Sundararajan, J.A.; Qiang, Y. Advanced nanomaterials for nuclear energy and nanotechnology. *Energy Technol.* **2020**, *8*, 1901070. [CrossRef]
13. Malekzadeh, R.; Sadeghi Zali, V.; Jahanbakhsh, O.; Okutan, M.; Mesbahi, A. The preparation and characterization of silicon-based composites doped with $BaSO^4$, WO^3, and PbO nanoparticles for shielding applications in PET and nuclear medicine facilities. *Nanomed. J.* **2020**, *7*, 324–334.
14. Singh, V.P.; Badiger, N.M.; Kaewkhao, J. Radiation shielding competence of silicate and borate heavy metal oxide glasses: Comparative study. *J. Non-Cryst. Solids* **2014**, *404*, 167–173. [CrossRef]
15. Mostafa, A.M.A.; Zakaly, H.M.; Pyshkina, M.; Issa, S.A.; Tekin, H.O.; Sidek, H.A.A.; Zaid, M.H.M. Multi-objective optimization strategies for radiation shielding performance of BZBB glasses using Bi^2O^3: A FLUKA Monte Carlo code calculation. *J. Mater. Res. Technol.* **2020**, *9*, 12335–12345. [CrossRef]
16. Çağlar, M.; Karabul, Y.; Kılıç, M.; Özdemir, Z.G.; İçelli, O. $Na^2Si^3O^7$/Ag micro and nano-structured glassy composites: The experimental and MCNP simulation surveys of their radiation shielding performances. *Prog. Nucl. Energy* **2021**, *139*, 103855. [CrossRef]
17. Allam, A.E.; El-Sharkawy, R.M.; El-Taher, A.; Shaaban, E.R.; Elsaman, R.; El Sayed Massoud, E.; Mahmoud, M.E. Enhancement and optimization of gamma radiation shielding by doped nano HgO into nanoscale bentonite. *Nucl. Eng. Technol.* **2022**, *54*, 2253–2261. [CrossRef]
18. Abdel Wahab, E.A.; Shaaban, K.S.; Elsaman, R.; Yousef, E.S. Radiation shielding and physical properties of lead borate glass-doped ZrO2 nanoparticles. *Appl. Phys. A* **2019**, *125*, 1–15. [CrossRef]
19. De Angelis, A.; Tatischeff, V.; Argan, A.; Brandt, S.; Bulgarelli, A.; Bykov, A.; Zoglauer, A. Gamma-ray astrophysics in the MeV range. *Exp. Astron.* **2021**, *51*, 1225–1254. [CrossRef]
20. Schimmerling, W.; Wilson, J.W.; Nealy, J.E.; Thibeault, S.A.; Cucinotta, F.A.; Shinn, J.L.; Kiefer, R. Shielding against galactic cosmic rays. *Adv. Space Res.* **1996**, *17*, 31–36. [CrossRef] [PubMed]
21. Goorley, T.; James, M.; Booth, T.; Brown, F.; Bull, J.; Cox, L.J.; Durkee, J.; Elson, J.; Fensin, M.; Forster, R.A.; et al. Is lead dust within nuclear medicine departments a hazard to pediatric patients? *J. Nucl. Med. Technol.* **2013**, *37*, 170–172.
22. Knoll, G. *Radiation Detection and Measurement*, 3rd ed.; John Wiley & Sons, Inc.: Hoboken, NJ, USA, 2000.
23. Berger, M.J.; Hubbell, J.H. XCOM: Photon Cross-Sections Database, Web Version 1.2 n.d. 2022. Available online: https://www.nist.gov/pml/productsservices/physical-reference-data (accessed on 27 December 2022).
24. Choppin, G.R.; Liljenzin, J.; Rydberg, J. Chapter 6–Absorption of Nuclear Radiation. In *Radiochemistry and Nuclear Chemistry Book*, 3rd ed.; 2002; pp. 123–165. Available online: https://www.sciencedirect.com/science/article/pii/B9780750674638500066 (accessed on 27 December 2022).
25. Gundogdua, O.; Tarimb, U.A.; Gurlerb, O. Monte Carlo calculations for photon attenuation studies on different solid phantom materials. In Proceedings of the 3rd International Conference on Computational and Experimental Science and Engineering, Banda Aceh, Indonesia, 11–12 October 2021.
26. Sayyed, M.I.; Mohammed, F.Q.; Mahmoud, K.A.; Lacomme, E.; Kaky, K.M.; Khandaker, M.U.; Faruque, M.R. Evaluation of radiation shielding features of Co and Ni-based superalloys using MCNP-5 code: Potential use in nuclear safety. *Appl. Sci. J.* **2020**, *10*, 7680. [CrossRef]